

IMPLICATION OF THE NON-DETECTION OF NEUTRINOS ABOVE 2PEV

LEE YACOBI

Department of Physics, Technion, Israel

DAFNE GUETTA

Osservatorio astronomico di Roma, v. Frascati 33, 00040 Monte Porzio Catone, Italy
Department of Physics Optical Engineering, ORT Braude, P.O. Box 78, Carmiel, Israel and
Department of Physics, Technion, Israel

EHUD BEHAR

Department of Physics, Technion, Israel

Draft version October 6, 2018

ABSTRACT

The IceCube telescope has detected diffuse neutrino emission, 20 events of which were reported to be above 60 TeV. In this paper, we fit the diffuse neutrino spectrum using Poisson statistics, which are the most appropriate for the low counts per energy bin. We extend the fitted energy range and exploit the fact that no neutrinos were detected above 2 PeV, despite the high detector sensitivity around the Glashow resonance at 6.3 PeV and beyond. A best-fit power-law slope of $\alpha = 2.9 \pm 0.3$ is found with no evidence for a high-energy cutoff. This slope is steeper than $\alpha = 2.3 \pm 0.3$ found by the IceCube team using a different fitting method. Such a steep spectrum facilitates the identification of high energy (\gg PeV) neutrinos, if detected, to be due to the GZK effect of cosmic-ray protons interacting with the Extragalactic Background Light. We use the ratio of EeV to PeV neutrinos in GZK models to show that the currently detected PeV neutrinos could not be due to the GZK effect, because this would imply many more higher-energy neutrinos that should have been detected, but were not. The non-detection of GZK neutrinos by IceCube despite more than essentially 1200 observing days, has already ruled out (at 95% confidence) models that predict rates of ~ 1 neutrino/yr or more. We use this non-detection to quantify the confidence at which GZK models are ruled out, and compute the additional IceCube and (in the future) ARA observing time that would rule them out with 95% confidence if no detection is made.

1. INTRODUCTION

IceCube, the km² neutrino detector in the south pole has detected 20 diffuse neutrinos above 60 TeV with the highest energy being $\sim 2 \pm 0.25$ PeV. These data were fitted by the IceCube Collaboration in the interval of $60 \text{ TeV} < E < 3 \text{ PeV}$ to a single power-law with a normalization of $1.5 \times 10^{-8} \text{ GeV cm}^{-2} \text{ s}^{-1} \text{ sr}^{-1}$ at 100 TeV, and a power law slope of 2.3 ± 0.3 (Aartsen et al. 2014a). Steeper spectral slopes of 2.4-2.6 are obtained (Aartsen et al. 2015a,b), when including neutrinos down to 25 TeV in the fit, and subtracting the atmospheric-neutrino model.

The effective area of IceCube has a sharp peak around the Glashow Resonance at 6.3 PeV (Glashow 1960). This makes IceCube particularly sensitive above the highest-detected neutrino energy. Moreover, the extremely-high-energy neutrino search method performed by the IceCube collaboration (Abbasi et al. 2010, 2011; Aartsen et al. 2013) indicates overall increase of effective area with energy $\propto E^{0.6}$. Nevertheless this search has not yet found any neutrino above 2 PeV.

Theoretical models predict ultra high energy neutrinos, especially due to the Greisen Ztsepin Kuzmin effect (GZK, Greisen 1966; Zatsepin & Kuz'min 1966). The GZK effect is the photo-hadron interaction between the Ultra-High-Energy Cosmic-Ray (UHECR) protons and the Extragalactic Background Light (EBL) photons. This interaction with the Cosmic Microwave Background

(CMB, the low frequency end of the EBL) produces a cutoff in the UHECR spectrum at $\sim 5 \times 10^{19} \text{ eV}$ that was observed by Abbasi et al. (2008) and Abraham et al. (2008).

According to the GZK photo-hadron decay scheme, neutrinos are produced with energy $\sim 5\%$ of the seed proton. The resulting ultra-high-energy neutrinos escape from the interaction zone (i.e., neutrino source). The flux of the GZK neutrinos strongly depends on the cosmic-ray composition and cosmological source evolution, which is why different models differ greatly in their neutrino flux prediction. While the IceCube non-detection of GZK neutrinos so far has already constrained many theoretical models (Aartsen et al. 2013), future neutrino observatories, and in particular the Askaryan Radio Array (ARA) is being build with the main goal of detecting these high-energy neutrinos. In the present work, we aim to quantify the confidence at which model families can be rejected, to anticipate the ARA neutrino detection rates, and to calculate the observing time without detection that would rule out the models with high confidence.

This paper is organized as follows: In Sec. 2 we present fits of different spectral models to the existing neutrino spectrum. Sec. 3 ascribes statistical validity to GZK models from the literature. Sec. 4 includes our discussion and conclusions.

2. SPECTRAL ANALYSIS

2.1. Method

We aim to fit the IceCube neutrino spectrum above 60 TeV with several models and in particular to exploit the fact that high energy neutrinos above 2 PeV were not detected. All neutrinos are assumed to be the genuine diffuse astrophysical signal, after all background counts have been subtracted. The neutrino number flux density per solid angle can be defined as:

$$\Phi = \frac{dN}{dE dt dA d\Omega} \quad (1)$$

We use a forward-folding algorithm to fit two types of models: a power law

$$E^2 \Phi = \Phi_0 \left(\frac{E}{100 \text{ TeV}} \right)^{2-\alpha} \quad (2)$$

and a power law with a cutoff at E_c

$$E^2 \Phi = \Phi_0 \left(\frac{E}{100 \text{ TeV}} \right)^{2-\alpha} \exp \left(-\frac{100 \text{ TeV} - E}{E_c} \right) \quad (3)$$

We multiply each model Φ with the IceCube effective area A^{eff} , which is averaged over 4π sr (Aartsen et al. 2014a). We integrate over energy and multiply by the exposure time Δt and the 4π sr field of view to obtain the model neutrino counts N

$$N = 4\pi \Delta t \int \Phi A^{\text{eff}} dE \quad (4)$$

which can then be compared with the observed spectrum.

The energy range we use is from 60 TeV to 10 PeV, in order to include the Glashow resonance at 6.3 PeV in the IceCube effective area. We use Cash (C-)statistics (Cash 1979), which is commonly used in astrophysics for low count rate data that is distributed according to Poisson statistics. The fitting procedure minimizes the C-statistic computed when comparing the observed spectrum with the folded model (Arnaud et al. 2015). This minimization does not take into account the data errors, which makes it suitable for low count rate (small error) data. This method allows to readily fit unbinned data, i.e. bins with one or zero counts (Cash 1979). We test different binning schemes from 0.01 dex to 0.2 dex, results of which are discussed below.

2.2. Results

The best-fit parameters of the power law with and without a cutoff are presented in Table 1. The Cash statistic is also listed in the last column of Table 1 to give an idea of the relative goodness of fit.

We find a slope of $\alpha = 2.9 \pm 0.3$, which is steeper by 2σ than the slope of 2.3 ± 0.3 found by Aartsen et al. (2014a), who use a different statistical fitting method. Aartsen et al. (2014a) unfolded the observed spectrum, assuming $\alpha = 2.0$ in each bin, and then fitted the unfolded spectrum, while we directly forward-fitted the model to the count spectrum (Sec. 2.1). The discrepancy may also be partially attributed to the different energy range of 60 TeV – 3 PeV used by Aartsen et al. (2014a), which does not include the Glashow resonance. When we fix the slope to be 2.3, and fit for the normalization only up

Model	$\Phi_0 \left[\frac{10^{-8} \text{ GeV}}{\text{cm}^2 \text{ s sr}} \right]$	α	$\log \left(\frac{E_c}{\text{GeV}} \right)$	Cash Rank
Aartsen et al. (2014a)	1.5	2.3 ± 0.3		57.8
Power Law (PL)	$2.2^{+0.9}_{-0.7}$	$2.9^{+0.3}_{-0.3}$		50.2
PL w/cutoff	$2.2^{+1.2}_{-0.9}$	$2.9^{+0.6}_{-0.4}$	> 6	50.2
$\alpha=2$ PL w/cutoff	$1.9^{+0.6}_{-0.5}$	2	5.9 ± 0.3	56
$E < 1 \text{ PeV}$ dataset	$2.3^{+1}_{-0.8}$	$3.6^{+0.7}_{-0.6}$		32

Table 1

Fitting parameters for the three models and IceCube results. The last row is a power-law model fitted to the data, but only up to 1 PeV.

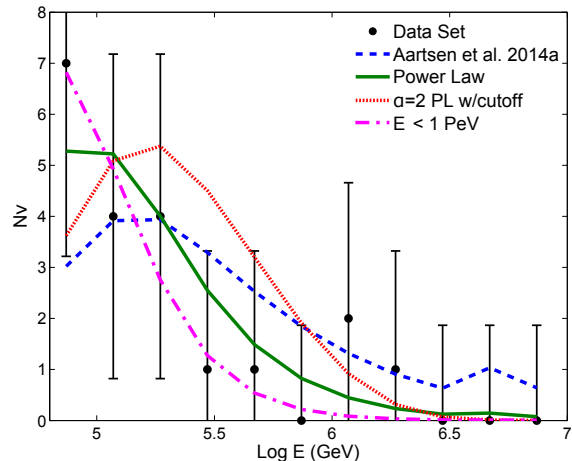


Figure 1. Observed neutrino spectrum compared with the various models (see Table 1). Data are binned to 0.2 dex. Poissonian errors of $1 + \sqrt{N + 0.75}$ (Gehrels 1986) are plotted just to guide the eye.

to 3 PeV, we find $\Phi_0 = 1.4 \pm 0.6$, which is indeed consistent with the Aartsen et al. (2014a) value of 1.5 (no uncertainty quoted).

We find no evidence for a cutoff in the data. Fitting for a cutoff results in $E_c > 1 \text{ EeV}$, which is far outside the fitted data range. The statistical uncertainty on E_c , however, is large; the fit only restricts E_c to be $> 1 \text{ PeV}$. In Table 1, we also show results for a power law and a cutoff, with the canonical slope of $\alpha = 2$ that might be motivated by theoretical cosmic-ray acceleration processes. In this case, the best-fit cutoff energy is at $\sim 1 \text{ PeV}$, but the fit is much worse.

It is evident from the IceCube data that no neutrinos were detected between 400 TeV and 1 PeV, with three neutrinos detected between 1–2 PeV. It has been suggested that the 17 neutrinos with $E < 400 \text{ TeV}$ and the three PeV neutrinos have different origins, e.g., dark matter annihilation (Murase et al. 2015). If we ignore the three PeV neutrinos and fit a power law model, the resulting slope of $\alpha = 3.6 \pm 0.7$ is much steeper than the slope obtained with the PeV neutrinos. The C-statistic is obviously much better as the PeV events, which are the least consistent with a power law, were removed.

In Fig. 1 we plot the neutrino data as well as the various models. It can be seen that on this plot the best-fitted power law model passes closer to the data points than any other model. This is due to the correct treatment of zero count bins. The fixed $\alpha = 2$ power law with a cutoff seems the least appropriate, likely implying that

Season	# Strings	A^{eff} (% of IC86)	Period (days)	IC86 equivalent (days)
May to May				
2010-2013	79-86	100	988	988
2008-2009	40	50	335	167
2007-2008	22	28	242	69
Total				1224

Table 2

IceCube seasons for which the EHE analysis was performed (Abbasi et al. 2010, 2011; Aartsen et al. 2013)

the diffuse neutrinos are not produced at the cosmic-ray acceleration sources, which is also consistent with the lack of a clear angular coincidence with astrophysical sources (Aartsen et al. 2014b). The differences between the other models are still very small.

Since the neutrinos do not always deposit all of their energy in the detector, some uncertainty can be associated with their energies. The actual neutrino energies are estimated to be $\sim 15\%$ greater than the deposited energy (Aartsen et al. 2014c). In order to test the effect of this uncertainty on the spectral parameters, we fitted the data using different bin sizes over a large range between 0.01 dex and 0.2 dex, which correspond to 2.3% – 45%, respectively, of the central energy in each bin. We find that using coarser bins makes no difference to the best-fitted spectral slope, which varies between $\alpha = 2.87 - 2.93$, and is totally consistent with 2.9 ± 0.3 obtained for unbinned data (Table 1). We conclude that the small uncertainty in neutrino energy makes no difference for constraining the spectral model parameters.

3. GZK NEUTRINOS

As shown in the previous section, the steep power law of the diffuse neutrinos implies a minute chance for detecting neutrinos above a few PeV. However, neutrinos at these energies are also expected to be produced by the photo-meson interaction of the EBL with high-energy cosmic rays at the Δ resonance (the GZK effect). In this section we examine several GZK neutrino models and calculate the number of neutrinos expected to be detected by current (IceCube) and future (ARA) neutrino telescopes. An analysis of signals from extremely-high-energy (EHE, $E > 10$ PeV) neutrinos including those produced outside of the detector, and exploiting the scaling of the effective area with energy approximately as $E^{0.6}$ significantly increases the sensitivity of IceCube to these EHE neutrinos (Abbasi et al. 2010, 2011; Aartsen et al. 2013). Next, we exploit the non-detection during previous IceCube seasons prior to the complete 86 string configuration (IC86). In Table 2 we show the three IceCube seasons, which add up to 1224 IC86-equivalent observing days. Despite this effort, no neutrino was detected above 2 PeV.

In order to test different GZK models from the literature we extracted model fluxes and similarly to Sec. 2.1 folded them through the instrument effective area to obtain neutrino counts. No τ neutrinos are expected from the GZK effect. However, the neutrinos oscillate between flavors to produce an equal flux density for each of the three flavors Φ_i^{obs} :

$$\Phi_i^{\text{obs}} = \frac{1}{3} (\Phi_e + \Phi_\mu) \quad (5)$$

where Φ_e and Φ_μ are the model electron and muon neu-

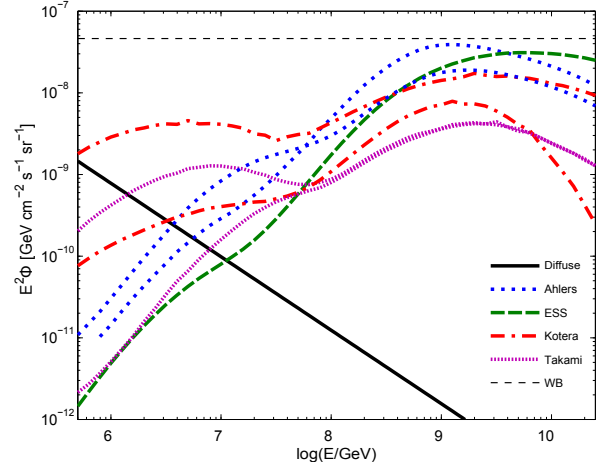


Figure 2. Various GZK neutrino models compared with the best-fitted diffuse flux model (Sec. 2) and with Waxman & Bahcall (1999). For each model we show the maximal and minimal predictions.

trino flux densities, respectively. Because of the Glashow resonance for $\bar{\nu}_e$ in IceCube, we compute the model fluxes separately for neutrinos and anti-neutrinos. Hence, Eq. 5 holds separately for anti-neutrinos as well. Since the flux density is the same for all flavors, we can sum the effective areas of all flavors

$$A^{\text{eff}} = \sum_{i=e,\mu,\tau} A_i^{\text{eff}} \quad (6)$$

and the same for anti-neutrinos. Finally, the prediction for the total number of neutrinos ($N_\nu + N_{\bar{\nu}}$) is obtained by adding the results of Eq. 4 for neutrinos and anti-neutrinos. The integration over energy in Eq. 4 is carried out from $E = 2$ PeV to 1 ZeV (10^{21} eV).

3.1. GZK models

The theoretical scheme of the GZK effect is an interaction of a UHECR proton with the EBL. The main channel for this interaction is the Δ -resonance:

$$p + \gamma \rightarrow \Delta^+ \rightarrow \begin{cases} n + \pi^+ \\ p + \pi^0 \end{cases} \quad (7)$$

In the case of protons in heavier nuclei, the efficiency of the interaction is reduced. The neutrino emission is due to pion decay

$$\pi^+ \rightarrow e^+ + \nu_e + \nu_\mu + \bar{\nu}_\mu \quad (8)$$

The resonance sets a requirement on $E_p E_\gamma$, so the proton energy required for the interaction decreases with redshift. The CMB photons interact with high energy protons producing a peak in the neutrino flux at $E_\nu \approx 5\% E_p \approx 10^9$ GeV, while shorter wavelength photons of the EBL interact with (more abundant) lower energy protons to produce neutrinos around $E_\nu \approx 10^6$ GeV. An additional minor contribution to the $\bar{\nu}_e$ flux comes from the neutron beta decay.

GZK models have been constrained based on IceCube data above 100 PeV (Aartsen et al. 2013). We use the non-detection of neutrinos above 2 PeV, but focus on

those models that are still marginally viable. The model families we consider here are Engel et al. (2001); Ahlers et al. (2010); Kotera et al. (2010); and Takami et al. (2009). These models span more than three orders of magnitude in neutrino flux, which covers the predictions of many other models (e.g., Protheroe & Johnson 1996; Kalashev et al. 2002; Ave et al. 2005; Aloisio et al. 2015). For the most part, the models differ by their assumptions on the cosmic-ray composition, mostly the Fe content, the spectrum, and on the cosmological (redshift) evolution of the EBL and UHECR sources. Figure 2 shows the neutrino flux predictions of four model families from the literature. For three of the models, we show the minimal and maximal neutrino flux ($E^2\Phi$) predictions. The figure also shows for reference the best-fit diffuse spectrum of Sec. 2 and the upper limit of Waxman & Bahcall (1999).

The models of Engel et al. (2001) assume only protons and employ the SOPHIA Monte Carlo code to simulate the full particle physics interactions between UHECR and the CMB, including multi-particle products, and not only the Δ resonance. They also consider different cosmic ray source evolutions. In Fig. 2 we plot the model with the mildest evolution with redshift (their Fig. 4), which yields the least number of neutrinos. The fact that they include only the CMB and not shorter wavelength background results in the low prediction of neutrinos around 10^{6-7} GeV. Their other models yield many more neutrinos above 3 PeV, which have not been detected. We use their distinction between ν and $\bar{\nu}$ when considering the detection numbers for IceCube.

The models of Ahlers et al. (2010) assume a pure proton cosmic-ray composition. An important parameter of this model is the energy at which the extragalactic cosmic rays dominate over the galactic component. It is the extragalactic component that produces neutrinos, and the transition energy (denoted there by E_{\min}) determines the minimum proton energy for the interaction. In Fig. 2 we plot the predictions of Ahlers et al. (2010) from their Fig. 4 using the full range of $10^{17.5} - 10^{19}$ eV for this parameter.

The models of Kotera et al. (2010) explore different cosmic-ray chemical compositions, different interacting proton energy ranges and spectra, and different cosmic-ray redshift evolution scenarios, including various transition energies between galactic and extragalactic cosmic-ray components. In Fig. 2 we plot the plausible flux range of Kotera et al. (2010, Fig. 9 therein), with parameters they consider reasonable.

Takami et al. (2009) assume only proton cosmic rays. Here we use only their scenario in which the cosmic ray ankle at 10^{19} eV is the extragalactic spectrum (dubbed there "proton dip" scenario). In Fig. 2 we plot the flux range of Takami et al. (2009) from their Fig. 4 (left hand side) that includes minimal proton energies of $10^7 - 10^9$ GeV.

Fig. 2 shows that all models predict a neutrino flux that is significantly above the diffuse spectrum at energies of $10^8 - 10^{10}$ GeV. As expected, the models of Kotera et al. (2010) and Takami et al. (2009) that include the IR and UV backgrounds produce a higher energy flux of neutrinos in the low-energy peak around 10^6 GeV.

4. DISCUSSION

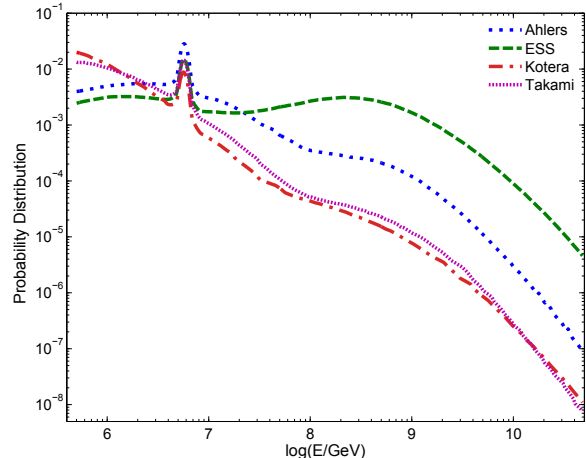


Figure 3. The neutrinos probability distribution function predicted by the various models for the IceCube effective area.

4.1. Origin of PeV Neutrinos

Since the GZK models have a significant peak at a few PeV (Fig. 2) that results from the EBL interaction with the UHECRs, one may wonder whether the three neutrinos detected by IceCube between 1 PeV - 2 PeV are actually GZK neutrinos, and not part of the diffuse power-law spectrum (Sec. 2). In Fig. 3 we show the probability distribution function of neutrinos ($\propto \Phi^{\text{model}} A^{\text{eff}}$) predicted by each type of GZK model to be observed in IceCube. Evidently, in all models, the number of neutrinos predicted to be detected up to 2 PeV is only a small fraction of the total predicted detections. The models that predict the strongest GZK neutrino effect at a few PeV are Kotera et al. (2010) and Takami et al. (2009). Even those two models predict IceCube would detect only $\approx 15\%$ of the neutrinos up to 2 PeV, and 85% above 2 PeV, implying that about twenty more neutrinos should have been observed at higher energies, but were not. This strongly suggests that the PeV neutrinos are not due to the GZK effect.

Roulet et al. (2013) reached the same conclusion by showing that model GZK neutrino fluxes are smaller than the observed flux at PeV energies. We strengthen this argument by demonstrating that the generic spectrum of GZK neutrinos, in which the flux of CMB-produced neutrinos (EeV) is higher than that produced (at PeV energies) by longer wavelength EBL, along with the increased detection efficiency of IceCube with energy, preclude the PeV neutrinos from being due to the GZK effect, regardless of the absolute flux of any specific model.

4.2. Constraining GZK Neutrino Models

We test the detectability of GZK neutrinos by calculating the number of detections expected from IceCube and from ARA using Eq. 4. In order to cover the entire energy range, we use the effective area for detecting contained neutrinos up to 10 PeV interacting inside the detector (Aartsen et al. 2014a), and higher energy (EHE) neutrinos, whose interaction starts outside the detector (Aartsen et al. 2013). It was noted by Karle (2010) that both effective area curves match at ~ 30 PeV. The resulting effective area curve multiplied by 4π (i.e., $\text{grasp} = A^{\text{eff}}\Omega$) is plotted in Fig. 4. The highest ARA curve for

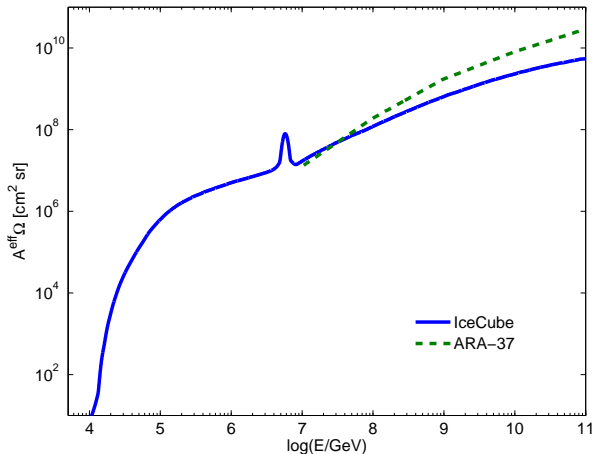


Figure 4. Effective Area times field of view of IceCube (grasp) with 86 strings and of ARA with 37 stations. Above the Glashow resonance, the IceCube effective area is for the EHE analysis method.

Model Family	IceCube	Rejection CL (%)	Time left for 95% CL Rejection (yrs)	
	N^{model} (1224 days)		IceCube	ARA
Kotera	0.6-2.6	45-93	14-0.56	9-3
Ahlers	1.59-2.9	79-94	3.3-0.1	3.1-1.5
ESS	0.91	60	8.5	2.2
Takami	0.35-0.66	30-48	27-13	14-12.8

Table 3

GZK neutrino numbers predicted by the models, and the respective confidence levels for their rejection. Last two columns give the time, after 2013 for IceCube, and from beginning of operations for ARA, that it would take to reject the models at 95%, given that no GZK neutrinos are detected.

$A^{\text{eff}}\Omega$ in Hong & Connolly (2012) is also plotted. Note that the difference in $A^{\text{eff}}\Omega$ between the two telescopes is less than an order of magnitude, even at the highest energies.

The results are listed in Table 3. The first column gives the number of IceCube neutrinos predicted by the various models from the actual observation time of IceCube to date. It can be seen that the models predict $N^{\text{model}} \approx 0-3$ detections, which allows to constrain their viability. In the second column, we show the confidence level (CL) at which the models can be rejected given that no events were detected. The background free CL is approximately $\text{CL}(\%) = 1 - \exp(-N^{\text{model}})$ (Astone & Pizzella 2000). We also compute the number of years that it would take IceCube and also ARA to reject the various models at 95% CL. This assumes no neutrinos are detected, and 330 operational days a year. The third column shows the additional observation time for IceCube while the fourth column lists the time for ARA.

The longer IceCube goes without detecting GZK neutrinos, the higher the statistical significance at which GZK models can be ruled out. Given that IceCube has been working for several years, all models that predicted detection rates of $\sim 1/\text{yr}$ or more are already excluded with high confidence ($> 95\%$). As can be seen from Table 3, the IceCube time required to seriously challenge most models is only a few years (two of which have passed). There are still several years before neutrino de-

tectors will be able to exclude the full range of each model family, but it is already possible to constrain the parameters inside each family. The first to be ruled out are models that include only protons and those that assume strong cosmological evolution of the UHECR sources (see also Aartsen et al. 2013), which predict the highest neutrino fluxes.

5. CONCLUSIONS

We have studied the diffuse neutrino flux detected by IceCube. In particular, we used the non detection of neutrinos above 2 PeV to constrain diffuse neutrino spectral models and found that the best fit is obtained with a power law index of $\alpha = 2.9 \pm 0.3$, which is steeper than 2.3 ± 0.3 found by IceCube. More recent works extending the fitted range down to 25 TeV already find steeper slopes (Aartsen et al. 2015a,b). Here we show that an extension to higher energies beyond the Glashow resonance further steepens the fitted slope.

We also use the lack of neutrino detection above 2 PeV to constrain and even reject several model families that have been suggested for neutrino fluxes expected from the GZK effect (so-called cosmogenic neutrinos). As more data are being collected, neutrino telescopes like IceCube and later ARA will allow to constrain the GZK models much better. These observational constraints will be useful to better understand the origin of the UHECRs, the cosmological evolution of the sources, their spectrum, and chemical composition.

We are grateful for insightful discussions with M. Ahlers, H. Landsman, G. Nir, and A. Dar. This research is supported by the I-CORE program of the Planning and Budgeting Committee and the Israel Science Foundation (grant numbers 1937/12 and 1163/10), and by a grant from Israel's Ministry of Science and Technology. D.G. is supported by a grant from the U.S. Israel Binational Science Foundation. E.B. has received funding from the European Unions Horizon 2020 research and innovation programme under the Marie Skłodowska-Curie grant agreement No 655324.

REFERENCES

- Aartsen, M. G., Abbasi, R., Ackermann, M., et al. 2013, Phys. Rev. D, 88, 112008
- Aartsen, M. G., Ackermann, M., Adams, J., et al. 2014a, Physical Review Letters, 113, 101101
- Aartsen, M. G., Ackermann, M., Adams, J., et al. 2014b, ApJ, 796, 109
- Aartsen, M. G., Abbasi, R., Ackermann, M., et al. 2014c, Journal of Instrumentation, 9, P03009
- Aartsen, M. G., Ackermann, M., Adams, J., et al. 2015, Phys. Rev. D, 91, 022001
- IceCube Collaboration, Aartsen, M. G., Abraham, K., et al. 2015, arXiv:1507.03991
- Abbasi, R., Abdou, Y., Abu-Zayyad, T., et al. 2011, Phys. Rev. D, 83, 092003
- Abbasi, R., Abdou, Y., Abu-Zayyad, T., et al. 2010, Phys. Rev. D, 82, 072003
- Abbasi, R. U., Abu-Zayyad, T., Allen, M., et al. 2008, Physical Review Letters, 100, 101101
- Abraham, J., Abreu, P., Aglietta, M., et al. 2008, Physical Review Letters, 101, 061101
- Ahlers, M., Anchordoqui, L. A., Gonzalez-Garcia, M. C., Halzen, F., & Sarkar, S. 2010, Astroparticle Physics, 34, 106

- ARA Collaboration, Allison, P., et al. 2012, *Astroparticle Physics*, 35, 457
- Aloisio, R., Boncioli, D., di Matteo, A., et al. 2015, arXiv:1505.04020
- Astone, P., & Pizzella, G. 2000, arXiv:hep-ex/0002028
- Ave, M., Busca, N., Olinto, A. V., Watson, A. A., & Yamamoto, T. 2005, *Astroparticle Physics*, 23, 19
- Cash, W. 1979, *ApJ*, 228, 939
- Engel, R., Seckel, D., & Stanev, T. 2001, *Phys. Rev. D*, 64, 093010
- Gehrels, N. 1986, *ApJ*, 303, 336
- Glashow, S. L. 1960, *Physical Review*, 118, 316
- Greisen, K. 1966, *Physical Review Letters*, 16, 748
- Hong, E., & Connolly, A. ELOG ARA,2012.
https://www.phys.hawaii.edu/eelog/ARA/120601_104113/ARA37_from_AraSim_060112.pdf.
- Kalashov, O. E., Kuzmin, V. A., Semikoz, D. V., & Sigl, G. 2002, *Phys. Rev. D*, 66, 063004
- Kalashov, O., & Troitsky, S. 2015, *Soviet Journal of Experimental and Theoretical Physics Letters*, 100, 761
- Karle, A., for the IceCube Collaboration 2010, arXiv:1003.5715
- Kotera, K., Allard, D., & Olinto, A. V. 2010, *J. Cosmol. Astropart. Phys.*, 10, 013
- Murase, K., Laha, R., Ando, S., & Ahlers, M. 2015, arXiv:1503.04663
- Protheroe, R. J., & Johnson, P. A. 1996, *Astroparticle Physics*, 4, 253
- Roulet, E., Sigl, G., van Vliet, A., & Mollerach, S. 2013, *J. Cosmol. Astropart. Phys.*, 1, 028
- Takami, H., Murase, K., Nagataki, S., & Sato, K. 2009, *Astroparticle Physics*, 31, 201
- Waxman, E., & Bahcall, J. 1999, *Phys. Rev. D*, 59, 023002
- Arnaud, K., Dorman, B. & Gordon, C. Xspec Manual 2015
<https://heasarc.gsfc.nasa.gov/xanadu/xspec/manual/XSappendixStatistics.html>.
- Zatsepin, G. T., & Kuz'min, V. A. 1966, *ZhETF Pisma Redaktsiiu*, 4, 114